

CLEARED  
FOR PUBLIC RELEASE  
PL/PA 16 DEC 96

Sensor and Simulation Notes

Note 134

July 1971

A Cylindrical Post Above a Perfectly Conducting Plate, I (Static Case)

by

Lennart Marin  
Northrop Corporate Laboratories  
Pasadena, California

Abstract

The induced charge distribution on a cylindrical post above a perfectly conducting plate is obtained when the post is immersed in a homogeneous electrostatic field parallel to the axis of the post.

The capacitance and mean charge separation of two identical cylindrical posts are calculated for different separations between the cylinders and different diameter-to-length ratios of the cylinders. The induced charge density on the end caps is also graphed for two values of the post's diameter-to-length ratio and for several values of the plate-to-post separation.

PL 96-0950

## I. Introduction

In previous notes<sup>(2,3,4)</sup> the electromagnetic interaction of a two-parallel-plate simulator and a post inside it has been studied. The present note and a subsequent one are devoted to a closer investigation into the case where the post is very close to one of the parallel plates.

From the theory of images it follows that instead of studying the interaction of a post and a ground plane we can study the electromagnetic interaction of two cylindrical posts. In this note we will study in detail the electrostatic interaction of two cylinders, whereas the dynamic interaction will be treated in a subsequent note. In addition to calculating the surface charge density induced by a homogeneous electric field on the post, we will calculate the capacitance and the mean charge separation of two identical right circular cylinders. These latter two quantities characterize the low-frequency behavior of two cylinders when they are used as an antenna.

In section II we formulate an integral equation for the charge density on two equal cylinders with a common axis. This integral equation is then solved numerically in section III by making use of the Gaussian quadrature formula. The numerical results are given in graphical form for (1) the capacitance of two cylinders, (2) the mean charge separation, and (3) the surface charge density and total charges on the end caps of the two cylinders.

## II. Integral Equation for the Charge Density

Consider two identical, perfectly conducting, charged cylinders,  $S_+$  and  $S_-$ , having a common axis and immersed in an electrostatic field (see figure 1). The potential,  $\phi(\underline{r})$ , outside the cylinders is given by

$$\phi(\underline{r}) = \phi^{\text{inc}}(\underline{r}) + \phi^+(\underline{r}) + \phi^-(\underline{r}) \quad (1)$$

where

$$\phi^\pm(\underline{r}) = \epsilon_0^{-1} \int_{S_\pm} G(\underline{r}, \underline{r}') \sigma_\pm(\underline{r}') dS'$$

$$G(\underline{r}, \underline{r}') = (4\pi |\underline{r} - \underline{r}'|)^{-1}$$

$\sigma_+(\underline{r})$  and  $\sigma_-(\underline{r})$  are the charge densities on  $S_+$  and  $S_-$ , respectively, and  $\phi^{\text{inc}}(\underline{r})$  is the potential of the incident field. In the  $\phi$ -symmetric case with two oppositely charged cylinders, (1) can be reduced to

$$\begin{aligned} \phi(\underline{r}) = \phi^{\text{inc}}(\rho, z) + (\pi\epsilon_0)^{-1} & \left[ \int_0^a L(\rho, z, \rho', d) \sigma(\rho', d) d\rho' \right. \\ & \left. + \int_d^b L(\rho, z, a, z') \sigma(a, z') dz' + \int_0^a L(\rho, z, \rho', b) \sigma(\rho', b) d\rho' \right] \quad (2) \end{aligned}$$

where

$$L(\rho, z, \rho', z') = N(\rho, \rho', z - z') - N(\rho, \rho', z + z')$$

$$N(\rho, \rho', \zeta) = \frac{1}{2} k(\rho/\rho')^{\frac{1}{2}} K(k)$$

$$k = \{4\rho\rho' / [(\rho + \rho')^2 + \zeta^2]\}^{\frac{1}{2}}$$

and  $K(k)$  is the complete elliptic integral of the first kind

$$K(k) = \int_0^{\pi/2} (1 - k^2 \sin^2 \phi)^{-1/2} d\phi.$$

The requirement that the potential be a constant,  $\pm \phi_0$ , on each cylinder gives us the following integral equation for the charge density

$$\begin{aligned} \phi_0 = \phi^{\text{inc}}(\rho, z) + (\pi \epsilon_0)^{-1} & \left[ \int_0^a L(\rho, z, \rho', d) \sigma(\rho', d) d\rho' + \int_d^b L(\rho, z, a, z') \sigma(a, z') dz' \right. \\ & \left. + \int_0^a L(\rho, z, \rho', b) \sigma(\rho', b) d\rho' \right], \quad (\rho, z) \in S_+ \end{aligned} \quad (3)$$

Putting  $\phi^{\text{inc}}(\rho, z) = 0$  and introducing the normalized charge density  $s(\rho, z)$ ,

$$s(\rho, z) = a\sigma(\rho, z) / (\epsilon_0 \phi_0) \quad (4)$$

we have

$$\begin{aligned} \int_0^a L(\rho, z, \rho', d) s(\rho', d) d\rho' + \int_d^b L(\rho, z, a, z') s(a, z') dz' \\ + \int_0^a L(\rho, z, \rho', b) s(\rho', b) d\rho' = \pi \end{aligned} \quad (5)$$

The capacitance,  $C$ , between the two cylinders is then given by

$$C = \epsilon_0 aS \quad (6)$$

where

$$S = \pi \int_0^a [s(\rho', d) + s(\rho', b)] \rho' d\rho' + \pi \int_d^b s(a, z') a dz'.$$

The mean charge separation of the two cylinders,  $h_a$ , is defined as

$$h_a = 2\pi S^{-1} \left\{ \int_0^a [ds(\rho', d) + bs(\rho', b)] \rho' d\rho' + \int_d^b z' s(a, z') a dz' \right\} \quad (7)$$

A knowledge of  $C$  and  $h_a$  enables us immediately to determine the low-frequency characteristics of the two cylinders when used as an antenna. The normalized capacitance,  $S$ , defined by (6) and the mean charge separation of the two cylinders are graphed in figures 2 through 5, from the numerical solution of (5) which will be discussed in the next section.

The charge distribution on two cylinders having no net charge but immersed in a homogeneous electrostatic field directed along the common axis of the two cylinders can be obtained by solving equation (3) with

$$\phi^{inc}(\rho, z) = zE_0$$

and

$$\int_{S_+} \sigma(\rho, z) dS = 0.$$

The normalized charge densities  $s_1(\rho)$  and  $s_2(\rho)$ , defined by

$$s_1(\rho) = (\epsilon_0 E_0)^{-1} \sigma(\rho, d)$$

$$s_2(\rho) = (\epsilon_0 E_0)^{-1} \sigma(\rho, b)$$

are graphed in figures 6 through 9 for various values of  $d/a$  and  $h/a = .1, .02$ . The normalized total charges on the end caps of the post,  $Q_1$  and  $Q_2$ , defined by

$$Q_n = 2\pi a^{-2} \int_0^a \rho s_n(\rho) d\rho, \quad n = 1, 2$$

are graphed in figures 10 through 11 for a wide range of values of  $d/a$  and  $h/a$ .

### III. Numerical Results

Equation (5) was solved numerically by making use of the Gaussian quadrature formula. For  $|\rho - \rho'_j| + |z - z'_j| \neq 0$  the integrals on the left hand side of (5) can be approximated by the following sums

$$\int_0^a L(\rho, z, \rho', d) \sigma(\rho', d) d\rho' \approx \sum_{j=1}^{N_1} L(\rho, z, \rho'_j, z'_j) s(\rho'_j, z'_j) w_j,$$

$$\rho'_j = a[1 + \xi_j(N_1)]/2, \quad z'_j = d, \quad w_j = ar_j(N_1)/2$$

$$\int_d^b L(\rho, z, a, z') \sigma(a, z') dz' \approx \sum_{j=N_1+1}^{N_1+N_2} L(\rho, z, \rho'_j, z'_j) s(\rho'_j, z'_j) w_j,$$

$$\rho'_j = a, \quad z'_j = d + [b - d][1 + \xi_{j-N_1}(N_2)]/2,$$

$$w_j = (b - d)r_{j-N_1}(N_2)/2$$

(8)

$$\int_0^a L(\rho, z, \rho', b) \sigma(\rho', b) d\rho' \approx \sum_{j=M}^N L(\rho, z, \rho'_j, z'_j) s(\rho'_j, z'_j) w_j,$$

$$\rho'_j = a[1 + \xi_{j-M+1}(N_3)]/2, \quad z'_j = b,$$

$$w_j = ar_{j-M+1}(N_3)/2$$

where

$$M = N_1 + N_2 + 1$$

$$N = N_1 + N_2 + N_3$$

The abscissas,  $\xi_j(n)$ , and weight factors,  $r_j(n)$ , in the Gaussian integration formula using  $n$  sample points on the interval  $(-1, 1)$  are given by<sup>(7)</sup>

$$P_n[\xi_j(n)] = 0$$

$$r_j(n) = 2/\{[1 - \xi_j^2][P_n'(\xi_j)]^2\}$$

where  $P_n(\xi)$  is the Legendre polynomial of degree  $n$ . Approximating the left hand side of (5) by the sums (8) and setting the sum thus obtained equal to  $\pi$  at  $N$  points  $(\rho_i, z_i)$  we form a system of equations for determining  $s(\rho, z)$  at  $N$  points  $(\rho_j', z_j')$ . Because  $L(\rho, z, \rho', z')$  has a logarithmic singularity at  $\rho - \rho' = z - z' = 0$  and because we want the set of points  $(\rho_i, z_i)$  to coincide with the set of sample points  $(\rho_j', z_j')$  in the Gaussian integration formula, we proceed as follows. For  $1 \leq i \leq N_1$ , we have

$$\int_0^a L(\rho_i, z_i, \rho', d) s(\rho', d) d\rho' = \int_0^a S(\rho_i, z_i, \rho', d) s(\rho', d) d\rho' + \int_0^a R(\rho_i, z_i, \rho', d) s(\rho', d) d\rho' \quad (9)$$

where

$$S(\rho, z, \rho', z') = -\frac{1}{2} \frac{\rho'}{\sqrt{(\rho+\rho')^2 + (z-z')^2}} \ln[(\rho - \rho')^2 + (z - z')^2]$$

$$R(\rho, z, \rho', z') = L(\rho, \rho', z, z') - S(\rho, \rho', z, z')$$

Note that  $R(\rho, z, \rho', z')$  is finite and

$$R(\rho, z, \rho, z) = \frac{1}{2} \ln 8\rho - N(\rho, \rho, 2z)$$

Moreover, assuming that

$$[s(\rho, z) - s(\rho', z')] \ln[(\rho - \rho')^2 + (z - z')^2] = 0$$

at  $\rho - \rho' = z - z' = 0$  we have approximately

$$\begin{aligned}
\int_0^a L(\rho_i, z_i, \rho', d) s(\rho', d) d\rho' &\approx \sum_{\substack{j \neq i \\ j=1}}^{N_1} L(\rho_i, z_i, \rho_j, z_j) s(\rho_j, z_j) w_j \\
&+ \left[ R(\rho_i, z_i, \rho_i, z_i) w_i + S_1(\rho_i) \right. \\
&\left. - \sum_{\substack{j \neq i \\ j=1}}^{N_1} S(\rho_i, z_i, \rho_j, z_j) w_j \right] s(\rho_i, z_i) \quad (10)
\end{aligned}$$

where

$$S_1(\rho) = \int_0^a \frac{-\rho'}{\rho + \rho'} \ln|\rho - \rho'| d\rho'$$

In the same way, we get for  $N_1 + 1 \leq i \leq N_1 + N_2$

$$\begin{aligned}
\int_d^b L(\rho_i, z_i, a, z) s(a, z) dz' &\approx \sum_{\substack{j \neq i \\ j=N_1+1}}^{N_1+N_2} L(\rho_i, z_i, \rho_j, z_j) s(\rho_j, z_j) w_j \\
&+ \left[ R(\rho_i, z_i, \rho_i, z_i) w_i + S_2(z_i) \right. \\
&\left. - \sum_{\substack{j \neq i \\ j=N_1+1}}^{N_1+N_2} S(\rho_i, z_i, \rho_j, z_j) w_j \right] s(\rho_j, z_j) \quad (11)
\end{aligned}$$

where

$$S_2(z) = \int_d^b \frac{-\ln|z-z'|}{\sqrt{4a^2 + (z-z')^2}} dz'$$

Thus, we can form the following system of algebraic equations for the integral equation (5)

$$\sum_{j=1}^N L_{ij} s_j = \pi, \quad 1 \leq i \leq N \quad (12)$$

where

$$L_{ij} = L(\rho_i, z_i, \rho_j, z_j) w_j, \quad j \neq i$$

$$L_{ii} = \begin{cases} R(\rho_i, z_i, \rho_i, z_i) w_i + S_1(\rho_i) - \sum_{\substack{j=1 \\ j \neq i}}^{N_1} S(\rho_i, z_i, \rho_j, z_j) w_j, & 1 \leq i \leq N_1 \\ R(\rho_i, z_i, \rho_i, z_i) w_i + S_2(z_i) - \sum_{\substack{j=N_1+1 \\ j \neq i}}^{N_1+N_2} S(\rho_i, z_i, \rho_j, z_j) w_j, & N_1 + 1 \leq i \leq N_1 + N_2 \\ R(\rho_i, z_i, \rho_i, z_i) w_i + S_1(\rho_i) - \sum_{\substack{j=1 \\ j \neq i}}^N S(\rho_i, z_i, \rho_j, z_j) w_j, & M \leq i \leq N \end{cases}$$

The system of equations (12) was solved on an electronic computer (CDC 6600). A comparison of our numerical results with Smythe's<sup>(5,6)</sup> was made and agreement within a relative error of  $10^{-4}$  was found for the capacitance of one isolated cylinder. The capacitance between two cylinders is graphed in figures 2 and 3. The dashed curves in figure 3 is the capacitance obtained from the Kirchoff formula given by<sup>(1)</sup>

$$S \approx \pi a/d + \ln[8\pi a(1 + h/d)/d] - 1 + (4\pi h/b)\ln(1 + b/h) \quad (13)$$

Figures 4 and 5 are plots of the mean charge separation of two cylinders. The charge density and total charges on the end caps when the two cylinders are immersed in an incident electrostatic field are plotted in figures 6 through 11.

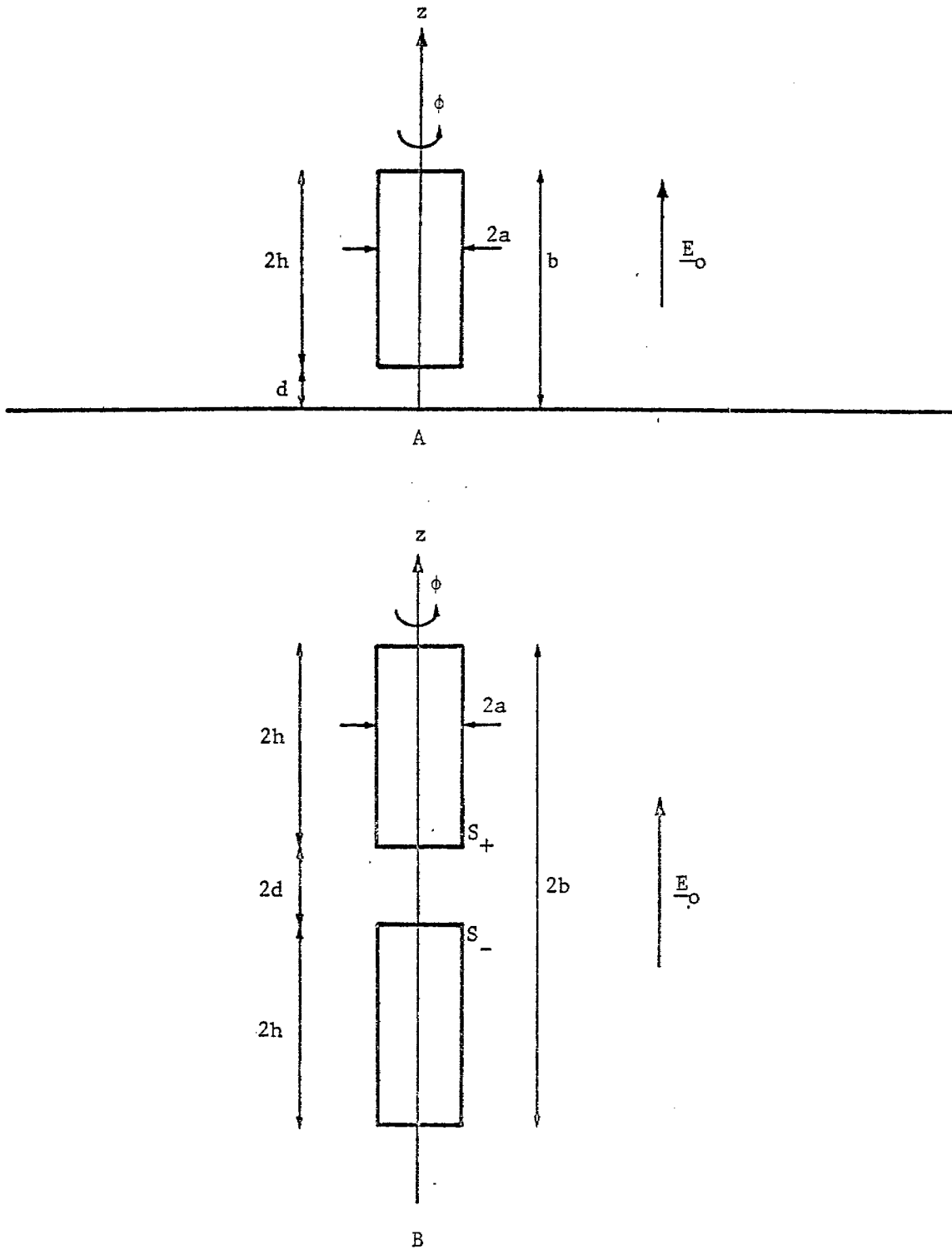


Figure 1. Electrostatic interaction of one cylindrical post and a perfectly conducting plane (A) and electrostatic interaction of two cylindrical posts (B): two equivalent situations.

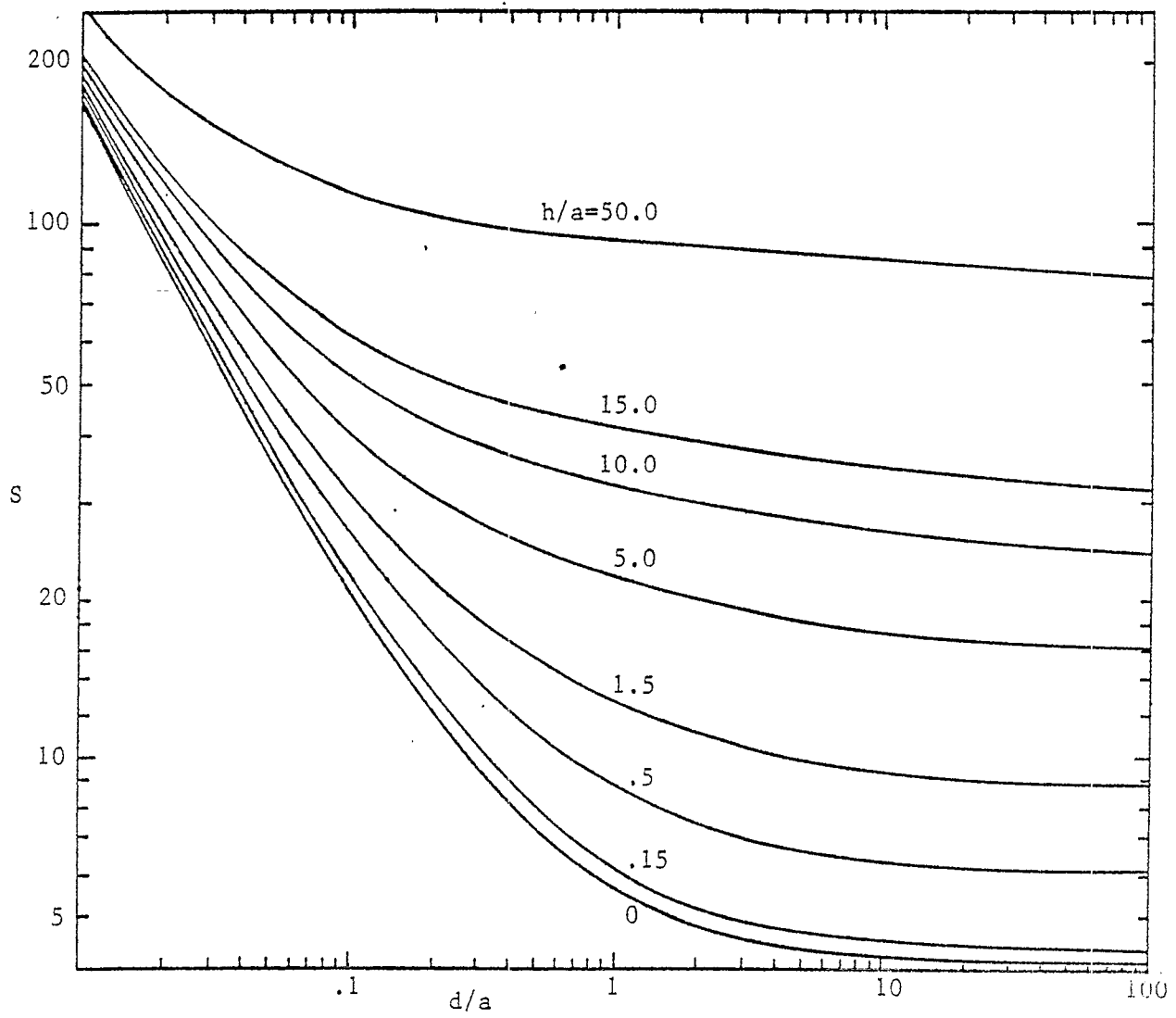


Figure 2. The capacitance of two cylinders.

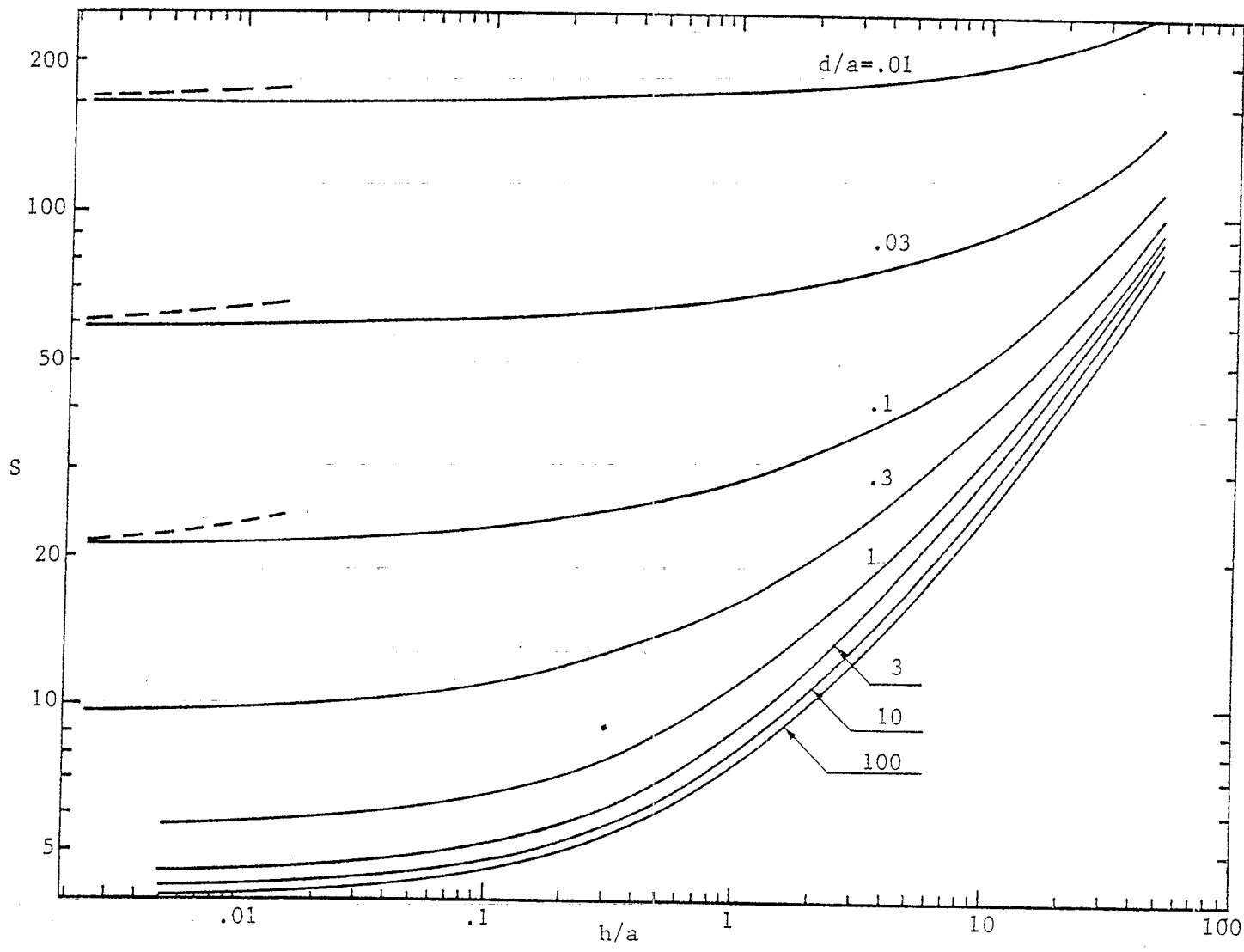


Figure 3. The capacitance of two cylinders.

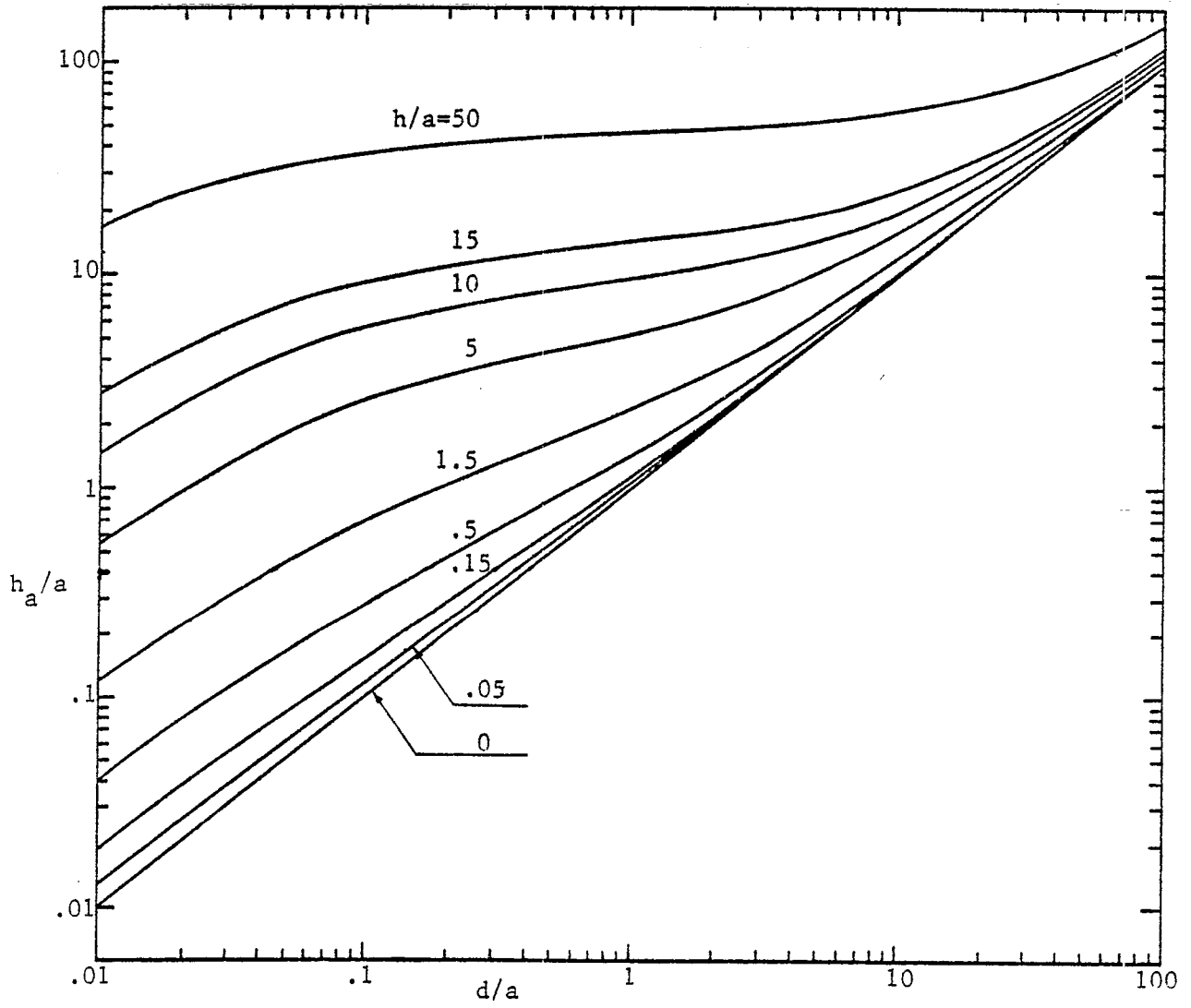


Figure 4. The mean charge separation of two cylinders.

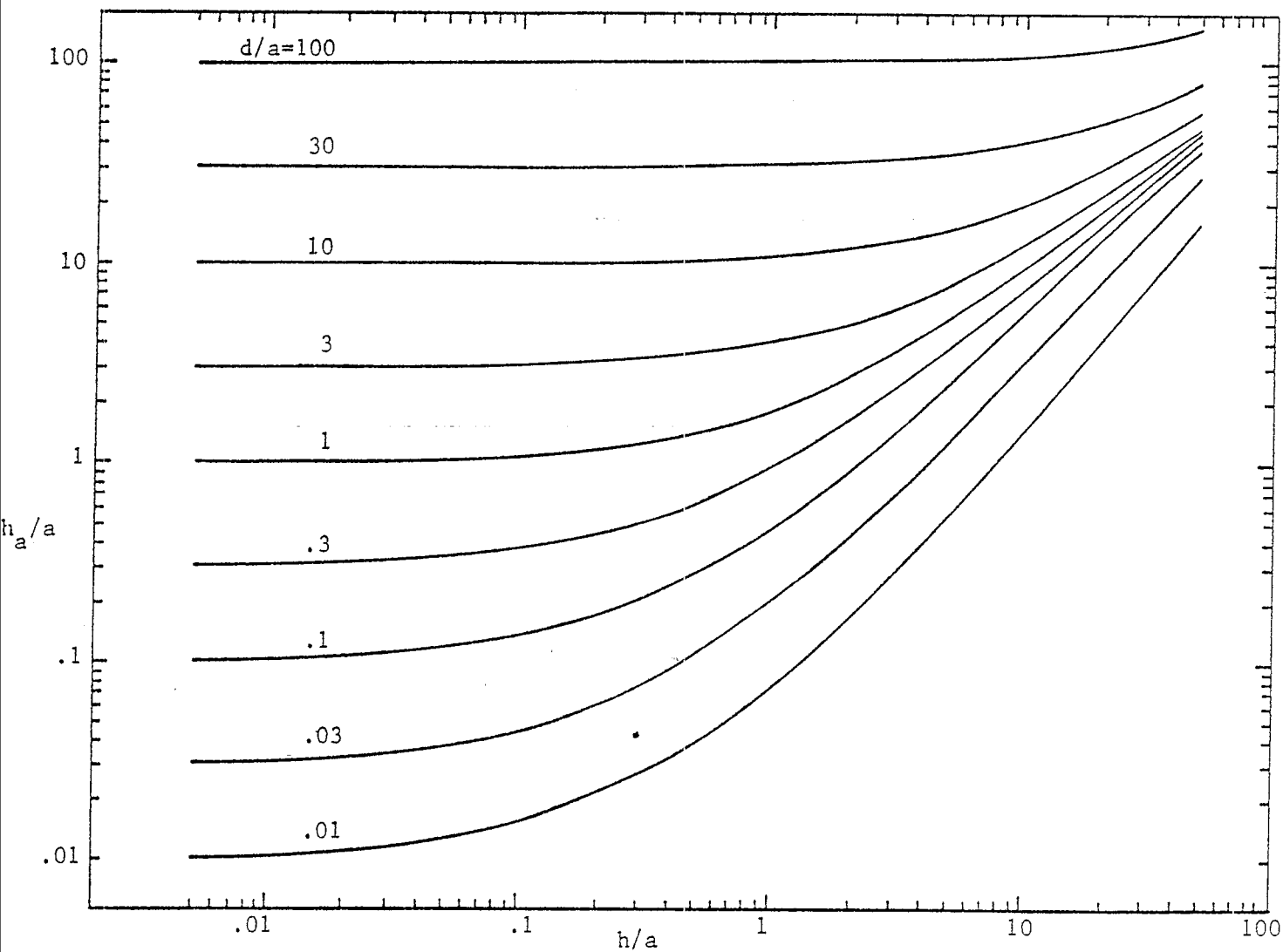


Figure 5. The mean charge separation of two cylinders.

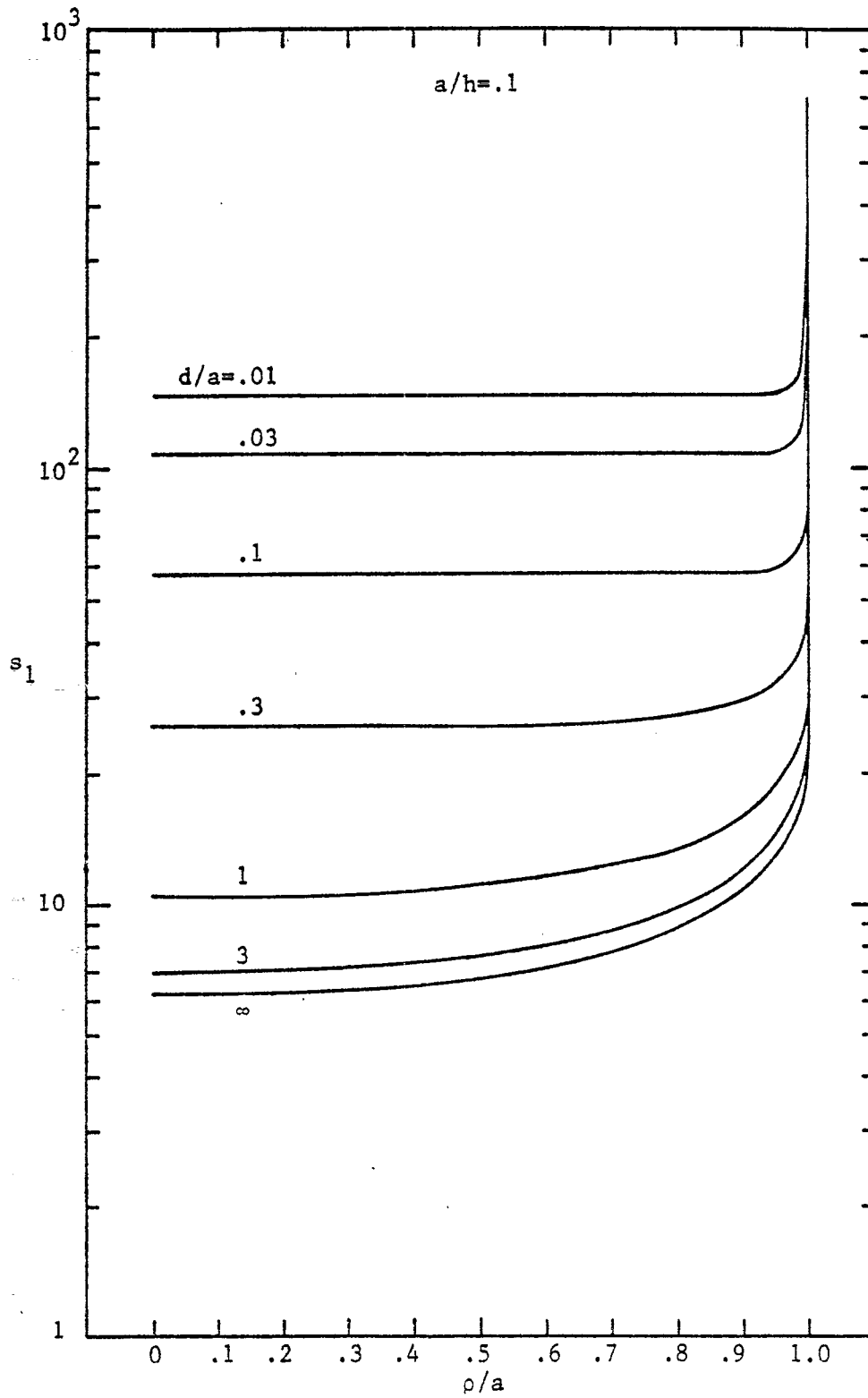


Figure 6. Charge distribution on the lower end cap of the cylinder.

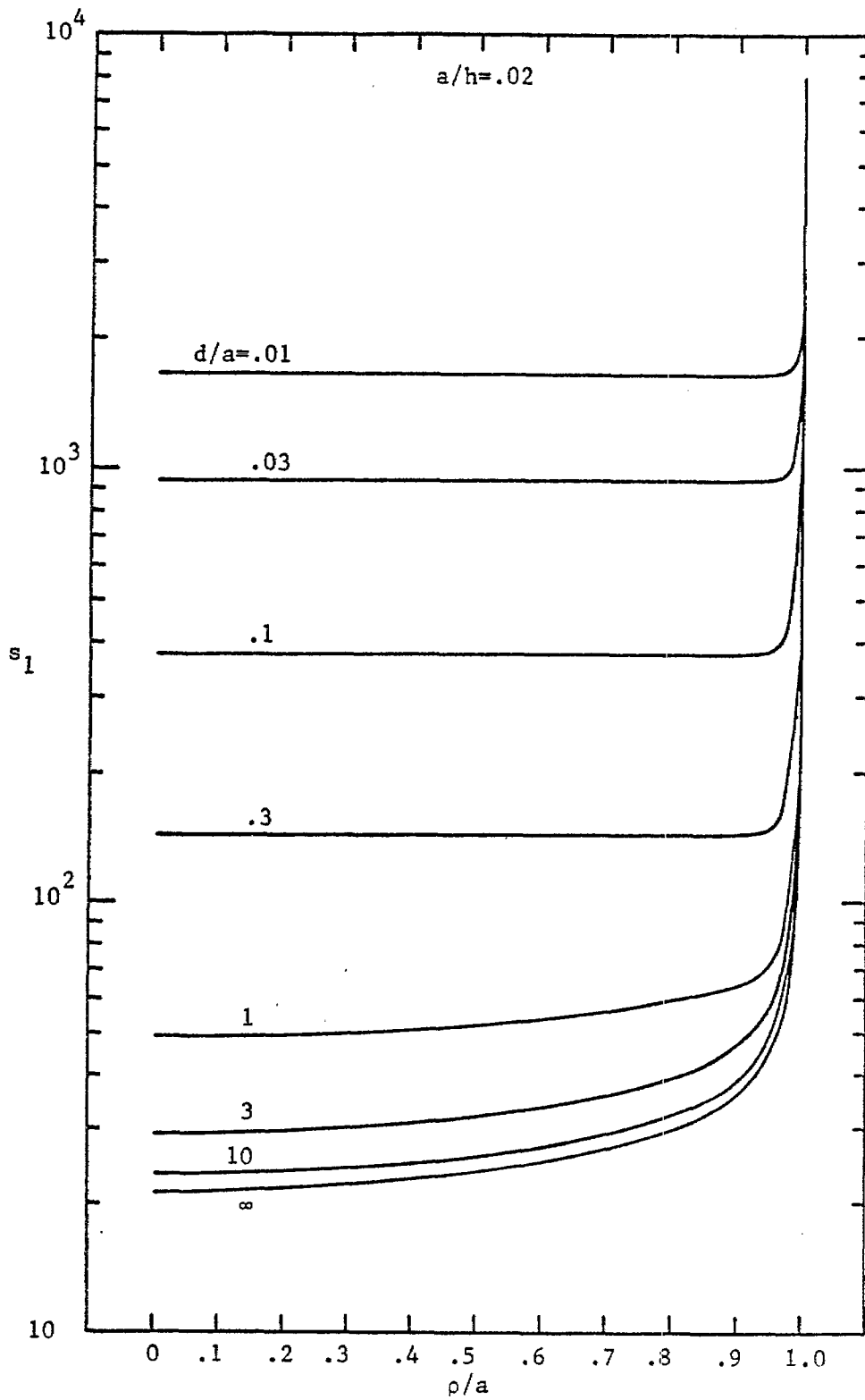


Figure 7. Charge distribution on the lower end cap of the cylinder.

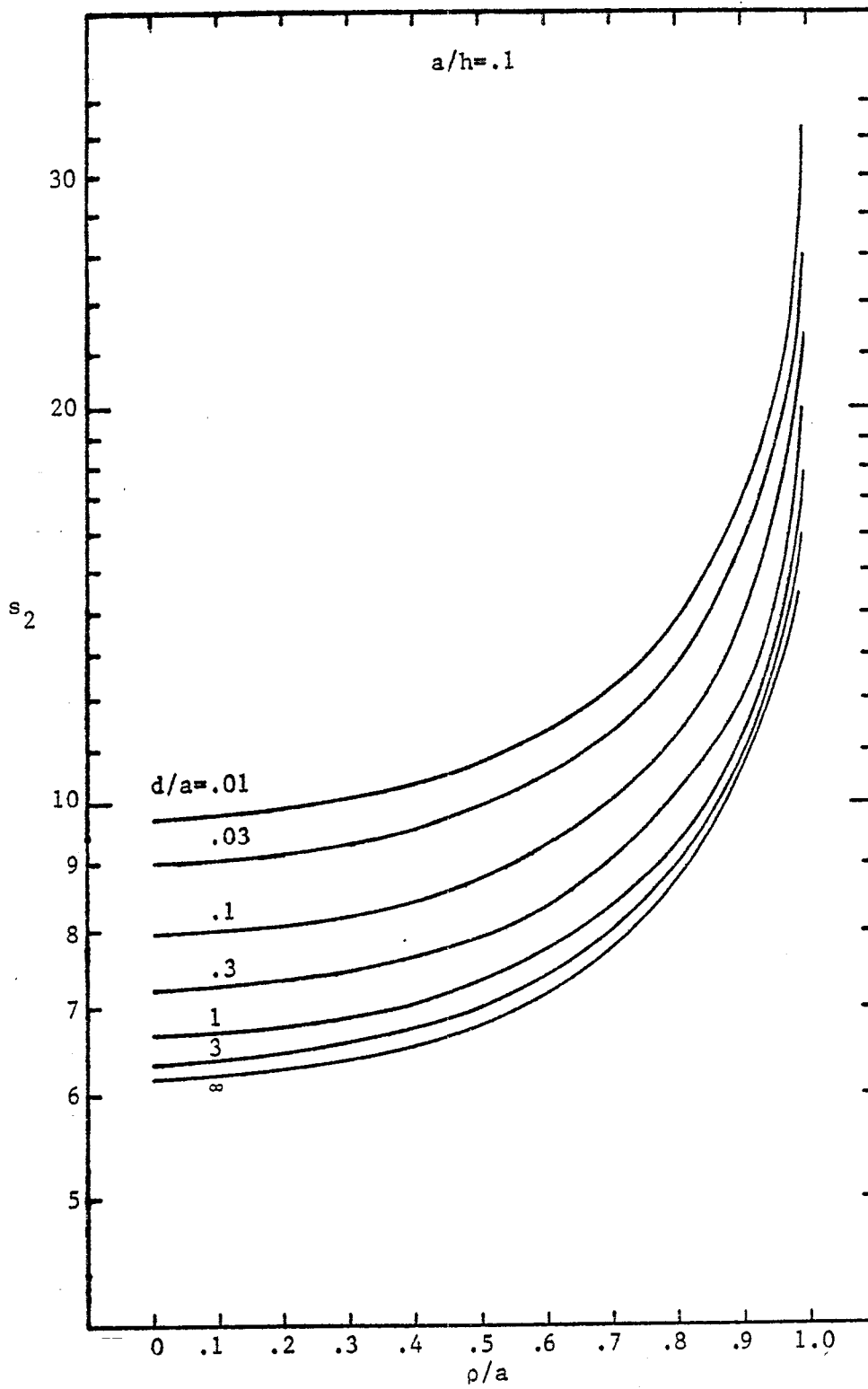


Figure 8. Charge distribution on the upper end cap of the cylinder.

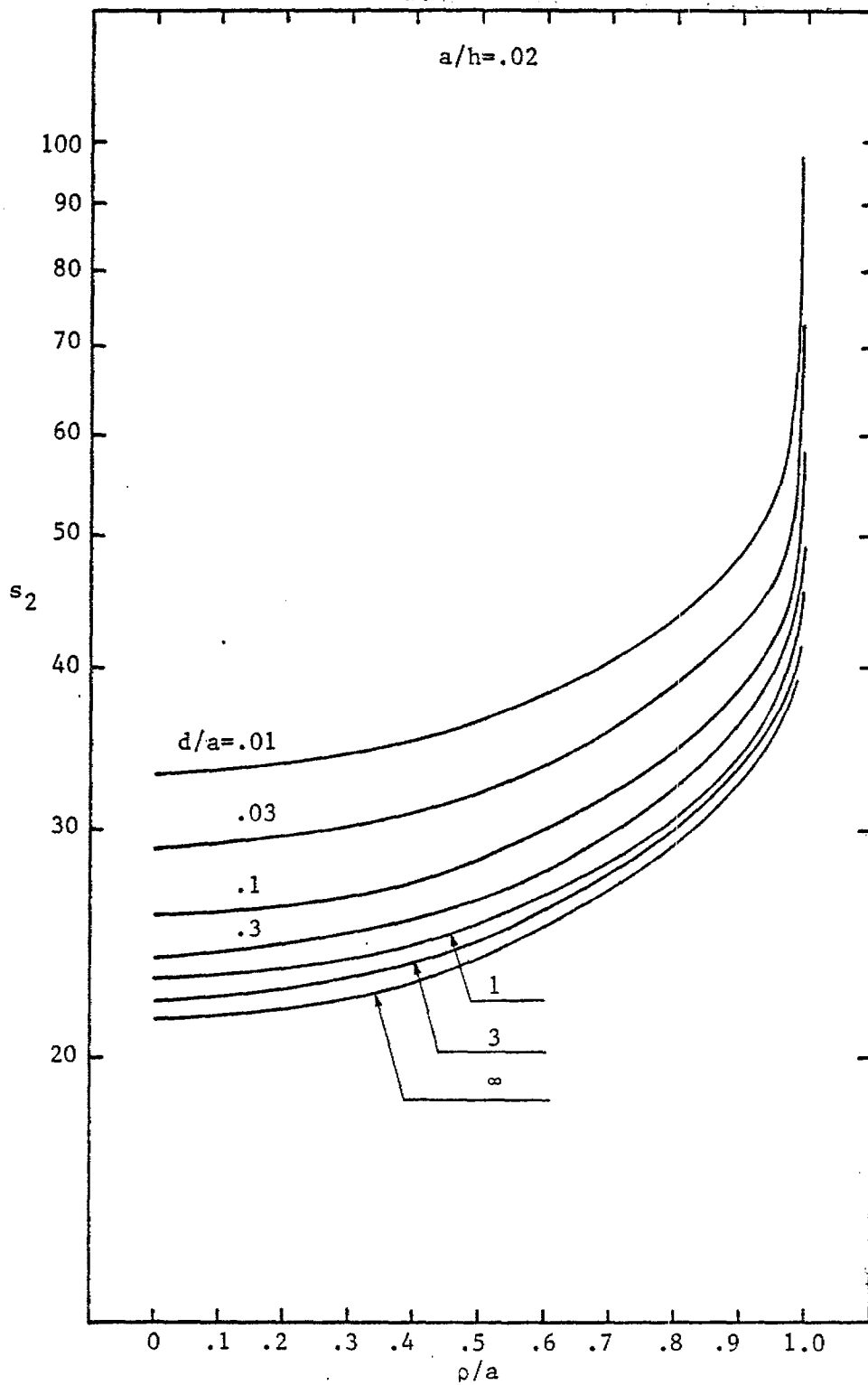


Figure 9. Charge distribution on the upper end cap of the cylinder.

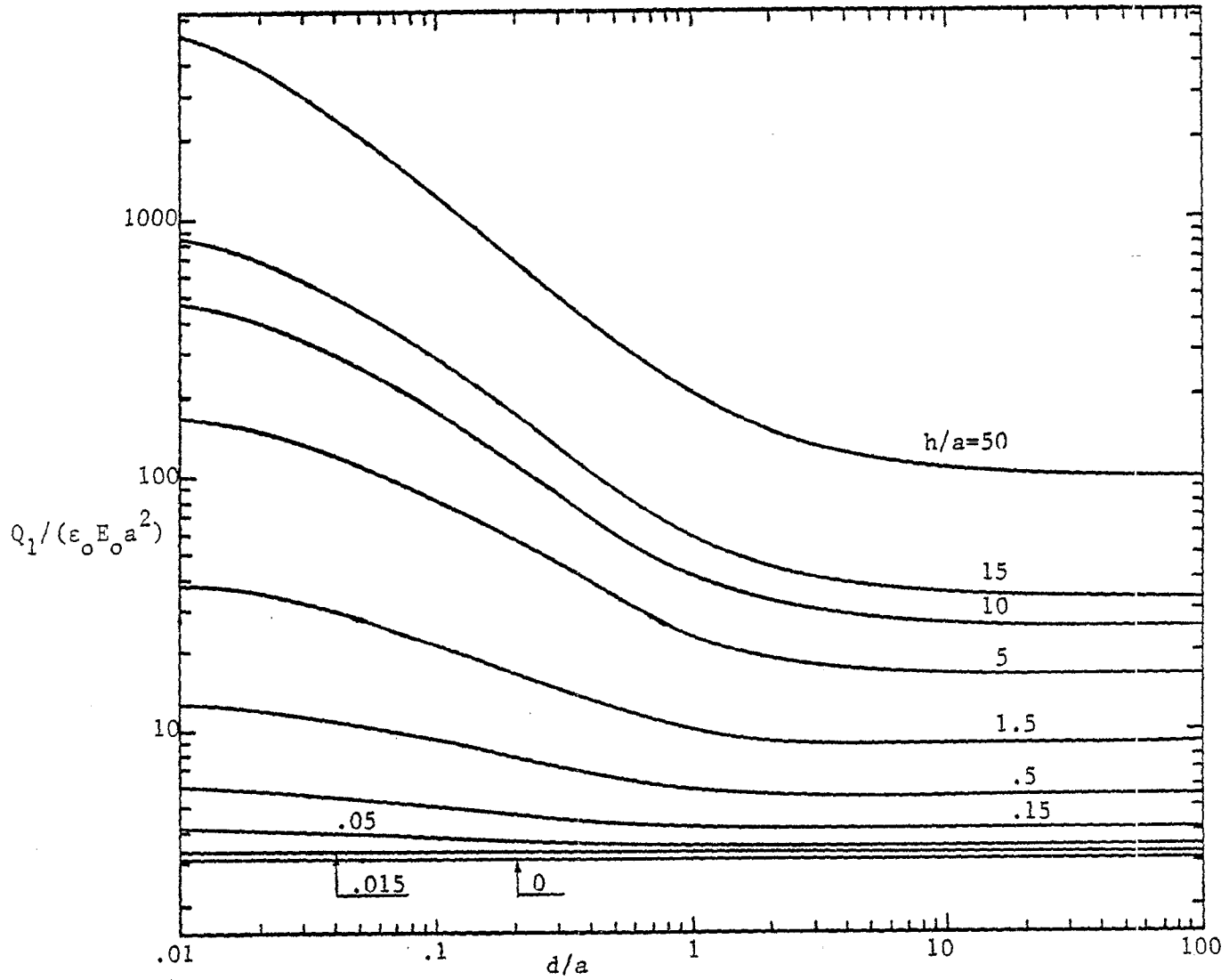


Figure 10. Total induced charge on the lower end cap of the cylinder.

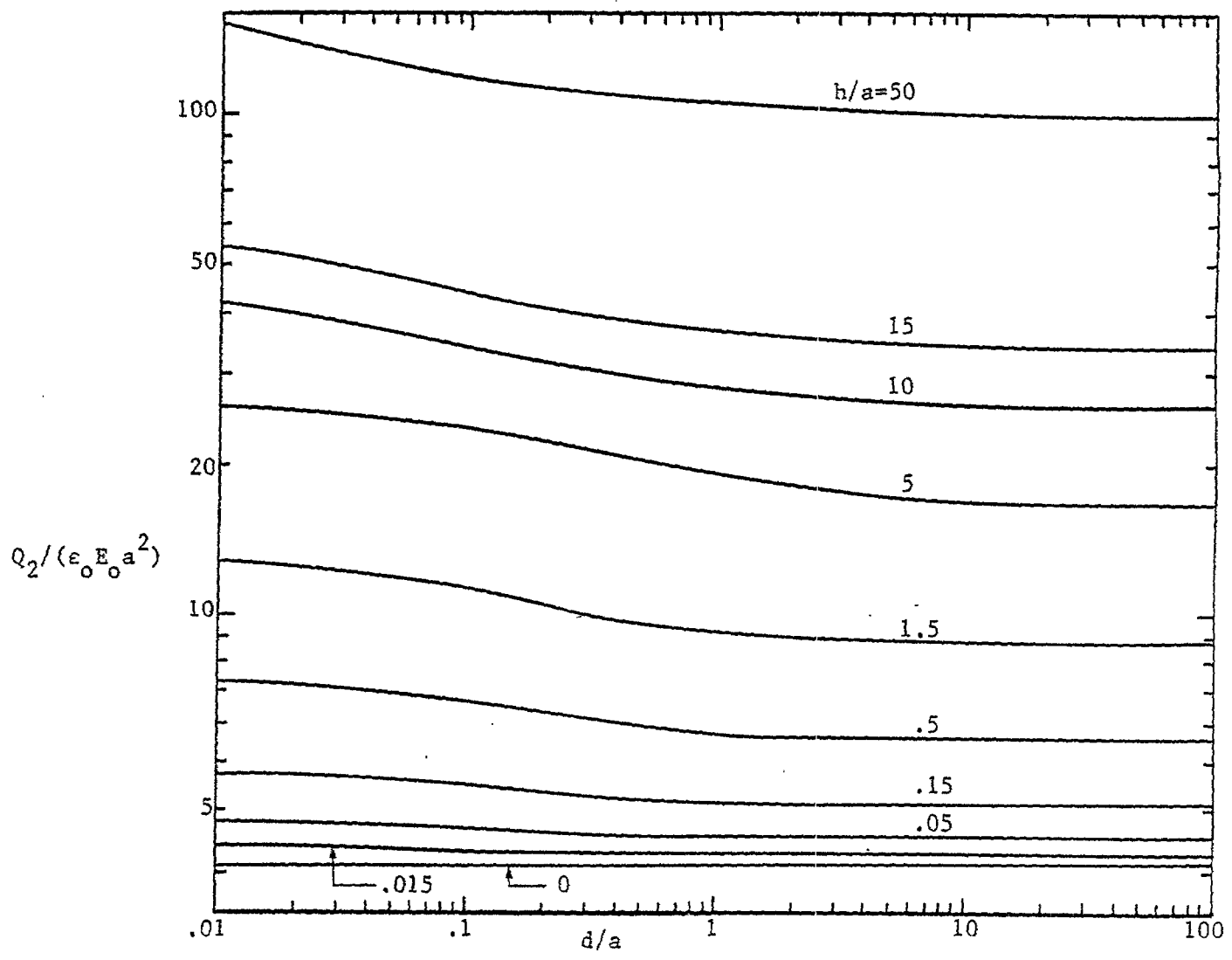


Figure 11. Total induced charge on the upper end cap of the cylinder

## Appendix

Although the capacitance of a freely charged right circular cylinder has been calculated by Smythe<sup>(5,6)</sup> and the electric polarizability tensor of a circular cylinder has been calculated by Taylor<sup>(7)</sup> we will here include some graphs and tables of the capacitance and induced charge on one cylinder. The following quantities have been calculated: (1) the equivalent radius,  $r_e$ , of a right cylinder defined as the radius of a sphere having the same capacitance,  $C$ , to infinity as a right cylinder, (2) the total charge,  $Q_o$ , induced on one end cap and (3) the charge density,  $s_o$ , at the center of each end cap when the cylinder is immersed in a homogeneous electric field,  $E_o$ , directed along the axis of the cylinder. In figure 12 we have graphed  $r_e$ ,  $r_e = C/(4\pi\epsilon_o)$ , as a function of  $h/a$ ,  $2h$  and  $a$  being the length and radius of the cylinder, respectively. Figures 13 and 14 are plots of  $Q_o/(\epsilon_o E_o a^2)$  and  $s_o/(\epsilon_o E_o)$ , respectively. In table 1 we have tabulated the same quantities as those graphed in figures 12-14.

Table 1

$h/a$	$r_e/a$	$Q_o/(\epsilon_o E_o a^2)$	$s_o$
0	.637	3.142	1.000
.005	.646	3.198	1.002
.015	.658	3.298	1.008
.050	.692	3.552	1.048
.150	.768	4.119	1.133
.500	.969	5.600	1.392
1.500	1.400	8.860	2.029
5.000	2.508	15.488	3.863
15.000	4.986	34.124	8.269
50.000	11.911	98.452	21.423

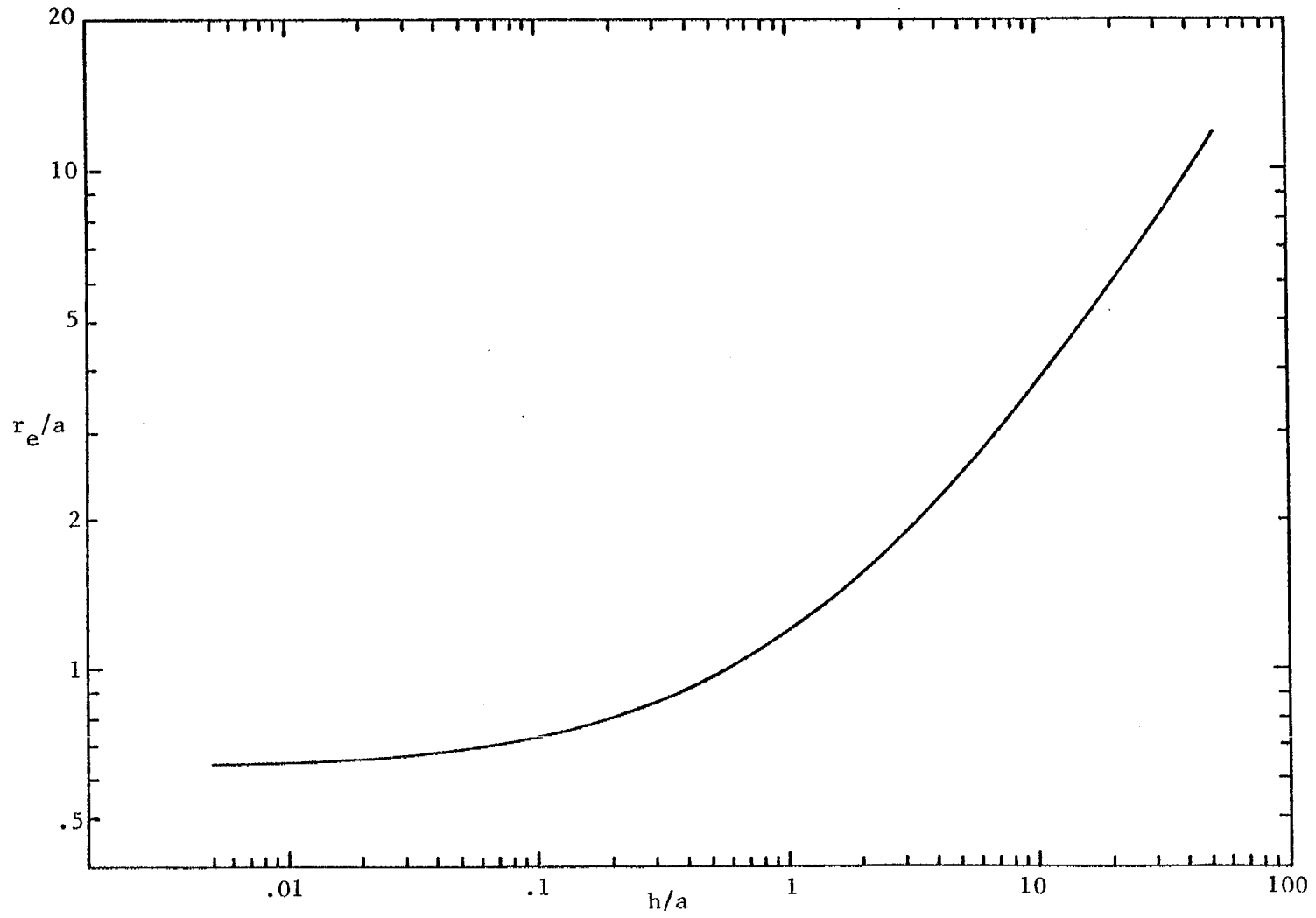


Figure 12. The equivalent radius of a right circular cylinder.

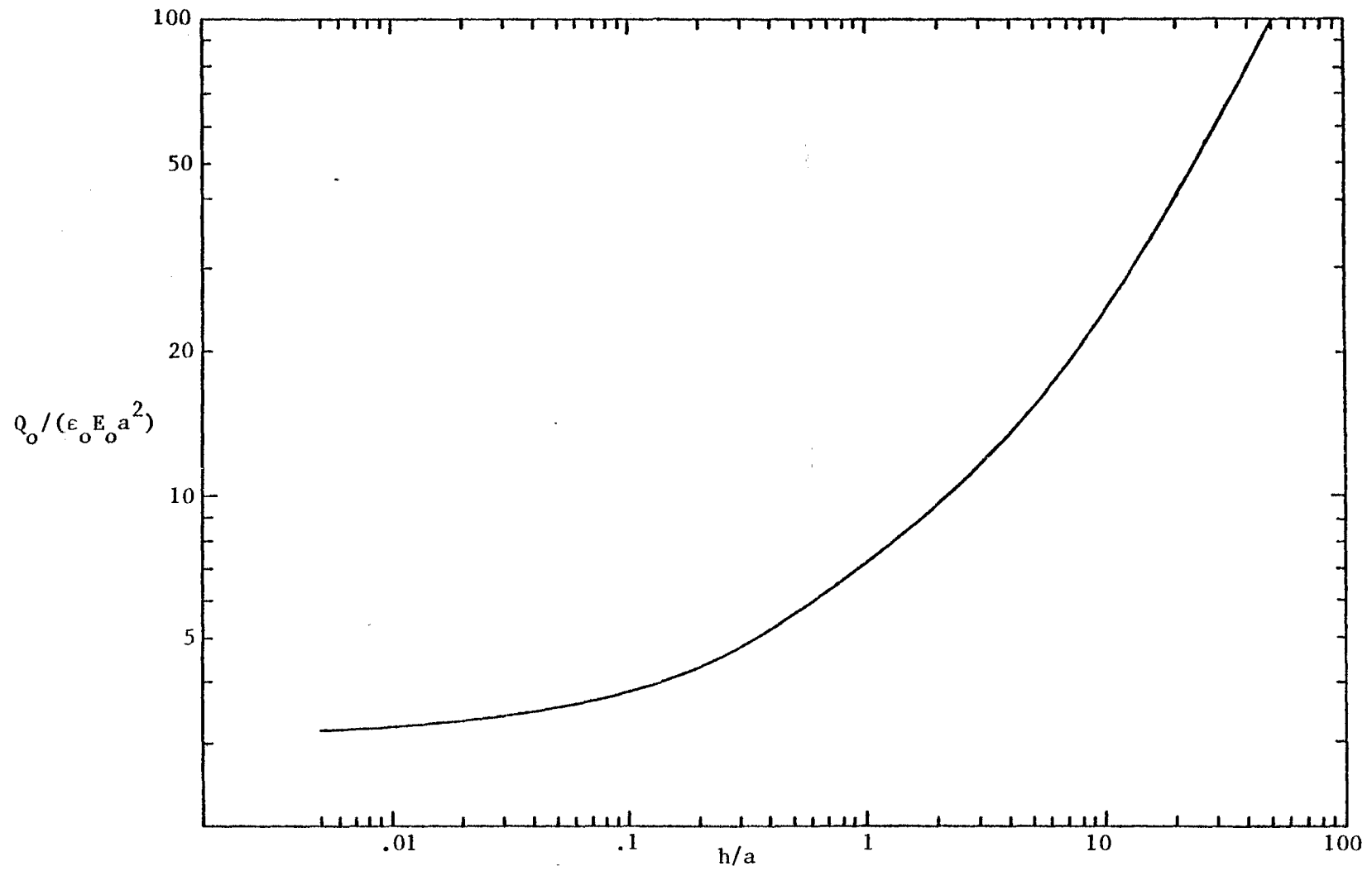


Figure 13. The total charge induced on one end cap.

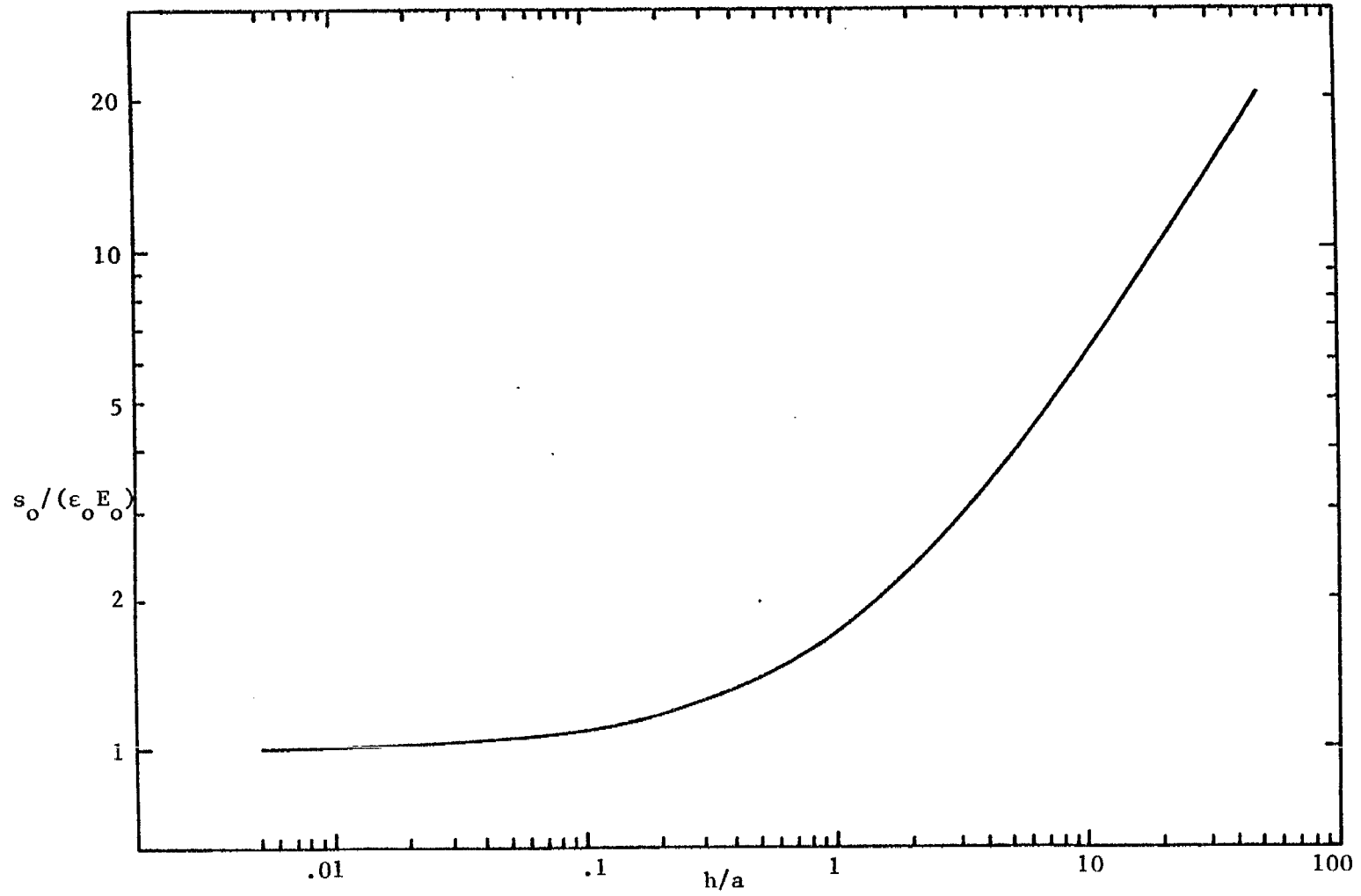


Figure 14. The induced charge density at the center of one end cap.

### Acknowledgment

We wish to thank Mr. R. W. Sassman for his numerical computations, Capt. C. E. Baum and Dr. K. S. H. Lee for their suggestions, and Mrs. G. Peralta for typing the manuscript and preparing the figures.

## References

1. C. E. Baum, "The Circular Parallel-Plate Dipole," Sensor and Simulation Note 80, March 1969.
2. R. W. Latham, K. S. H. Lee, and R. W. Sassman, "Minimization of Current Distortion on a Cylindrical Post Piercing a Parallel-Plate Waveguide," Sensor and Simulation Note 93, September 1969.
3. R. W. Latham and K. S. H. Lee, "Electromagnetic Interaction Between a Cylindrical Post and a Two-Parallel-Plate Simulator, I," Sensor and Simulation Note 111, July 1970.
4. K. S. H. Lee, "Electromagnetic Interaction Between a Cylindrical Post and a Two-Parallel-Plate Simulator, II (a Circular Hole in the Top Plate)," Sensor and Simulation Note 121, November 1970.
5. W. R. Smythe, "Charged Right Circular Cylinder," J. Appl. Phys., Vol. 27, No. 8, pp. 917-920, 1956.
6. W. R. Smythe, "Charged Right Circular Cylinder," J. Appl. Phys., Vol. 33, No. 10, pp. 2966-2967, 1962.
7. T. T. Taylor, "Electric Polarizability of a Short Right Circular Conducting Cylinder," J. Res. NBS, Vol. 64B, No. 3, pp. 135-143, 1960.
8. C. E. Fröberg, Introduction to Numerical Analysis, Addison-Wesley, New York, Second Edition, 1969.
9. M. Abramowitz and I. N. Stegun, Editors, Handbook of Mathematical Functions, National Bureau of Standards, AMS-55, 1964.